Chalcogenide Letters Vol. 6, No. 12, December 2009, p. 723-731

ELECTRICAL STUDY OF THIN FILM Al/n-CdS SCHOTTKY JUNCTION

SANDHYA GUPTA*, DINESH PATIDAR, N. S. SAXENA,
KANANBALA SHARMA
Semiconductor & Polymer Scince Laboratory, 5-6 Vigyan Bhawan, Dept. of Physics,University of Rajasthan, Jaipur, India

A study has been made on the behaviour of Al/n-CdS thin film junction on Polyethylene terephthalate (PET) grown using thermal evaporation method. I-V characteristics of this junction show that the Al makes Schottky contact with n-CdS. Intrinsic and contact properties such as saturation current, barrier height, ideality factor and series resistance were calculated from the I-V characteristics. The conduction seems to be predominantly due to thermoionic emission-diffusion mechanism. An effort has also been made to carry Optical study of CdS thin film was also carried out using spectrophotometer. Band gap of n-CdS thin film is determined through absorption spectra using the Tauc's extrapolation. A band diagram of Al/n-CdS has been proposed using the so obtained data.

(Received December 1, 2009; accepted December 22, 2009)

Keywords: Polyethylene terephthalate, I-V characteristics, Band gap, Schottky junction, Barrier hgight

1. Introduction

In metal-semiconductor junctions, prominent semiconductors are CdS, CdSe, which exhibit good interface behaviour. Cadmium sulfide (CdS) is a potential candidate in opto-electronic devices due to their good optical and electrical properties [1, 2]. CdS thin films can be prepared by different techniques such as thermal evaporation, close spaced sublimation, metal organic chemical vapour deposition (MOCVD), molecular- beam epitaxy (MBE), chemical bath deposition (CBD), chemical spray pyrolysis (CSP), electrodeposition and sputtering [3-8]. Among these methods thermal evaporation is one of the suitable method for depositing large area thin film for solar cell application. The development of CdS films on flexible substrates is gaining interest due to the light weight and damage free nature of the devices. Light weight CdS solar cells on flexible polymer substrates can be attractive for space applications [9].

Metal/CdS interfaces play an important role in optoelectronic device such as solar cells [9]. A clear understanding of the physical principles underlying the properties of these interfaces is therefore essential in order to develop practical devices based on this semiconductor material. Thus efforts have been made to study the properties of the interfaces through the measurements of I-V characteristics in Au-CdS junction by Chavez et al [2] and by Patel et al [10]. Also electrical studies have been made by Gupta et al [1] for Cu-CdS and Zn-CdS Schottky junctions by determining various junction parameters. However, very little efforts have been made in order to studying the properties of interfaces in the case of Al/CdS junction.

In view of this, in the present study Al/n-CdS junction is fabricated using thermal evaporation method on Polyethylene terephthalate (PET) substrate to get a flexible Schottky junction. Analysis of current–voltage (I–V) characteristics of this Schottky junction allows us to understand different aspects of current transport. The junction parameters such as barrier height, ideality factor, series resistance and saturation current have also been calculated from I–V characteristics of this junction at room temperature.

*corresponding email: 1982sanman@gmail.com, n_s_saxena@rediffmail.com

2. Experimental

2.1Thin film junction preparation

CdS thin film of area 2.25 cm^2 was prepared on PET substrate using evaporation of CdS powder (99.999% pure, from Alfa Aesar) in a residual pressure of 10^{-5} Torr. Cleaned PET film of 20 μm (from Good Fellow Cambridge Limited, England) thick was used as substrate and molybdenum was used as boat source. The thickness of CdS film is of the order of 300 nm, which was measured by Quartz crystal thickness monitor (Model CTM 200). After the deposition of CdS film over PET substrate, an aluminium film of area 0.5625 cm^2 is deposited over the CdS film just by breaking the vacuum in the chamber and then again restoring it to 10^{-5} Torr for the deposition of aluminium film. The thickness of Al-film deposited over the CdS film is 100 nm. Indium electrodes have been fabricated over CdS and aluminium films to be used as electrical contacts as shown in figure 1.

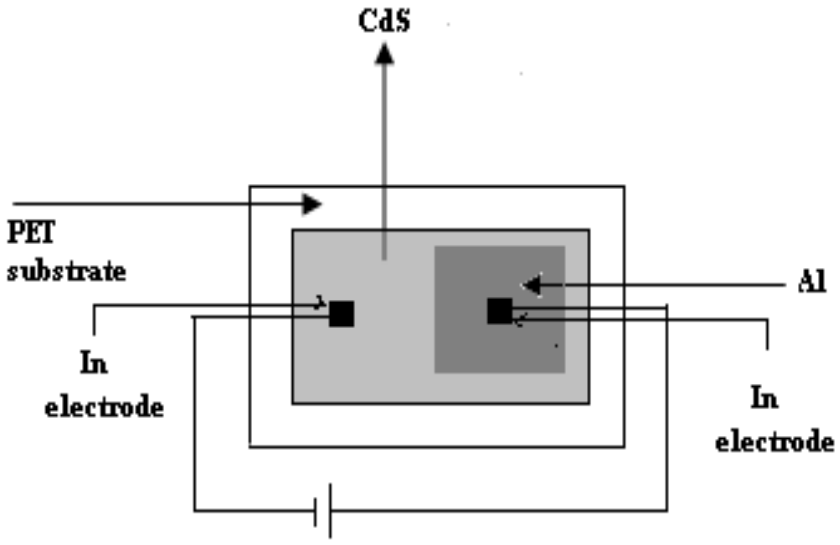

Fig. 1. Schematic diagram of Al/n-CdS junction

2.2 Techniques of characterization studies

Structural study of CdS-PET film was done using X-ray diffraction pattern performed with Philips X'pert X– ray diffractometer at a scanning rate of 3° per minute between 10 to 60°. The source used throughout this study was Cu, Kα (λ = 1.5406Å) operated at 40 mA and 45 kV.

I-V characteristics of Al/n-CdS Schottky junction were carried out by Keithley Electrometer/High Resistance meter 6517 A at room temperature. The electrical contacts were made on indium electrodes. Keithley Electrometer has an in built capacity of output independent voltage source of ±1000 volt. The voltage is applied across the sample to measure the current through the sample.

The optical absorption spectra of CdS thin film was recorded over the wavelength range 375 to 575 nm using an USB 2000 spectrophotometer at room temperature. In this spectrophotometer, absorption spectra are obtained directly through the computer using OOI Base 32 software. The light source is a deuterium lamp. Light falling on the sample is normal to the surface of film. From the absorption spectra, the optical band gap of CdS thin film was determined.

3. Results and discussion

Figure 2 shows the X-ray diffraction patterns of PET and CdS-PET films. These patterns show the semicrystalline nature of PET film and also contain a peak of CdS material in CdS-PET film. It reveals that CdS has hexagonal structure with primitive lattice having cell parameters of a = 4.136Å, c = 6.713Å and preferred (103) orientation of micro crystallites. The grain size of the crystallites (G) has been estimated using the following relation [11]:

$$G = k\,\lambda/(\beta \cos\theta) \quad (1)$$

where k is shape factor (≈1), λ is the wavelength of X-ray used, θ is Bragg's angle and β is the FWHM of the peak. The grain size of CdS particle is found to be of the order of 17 nm.

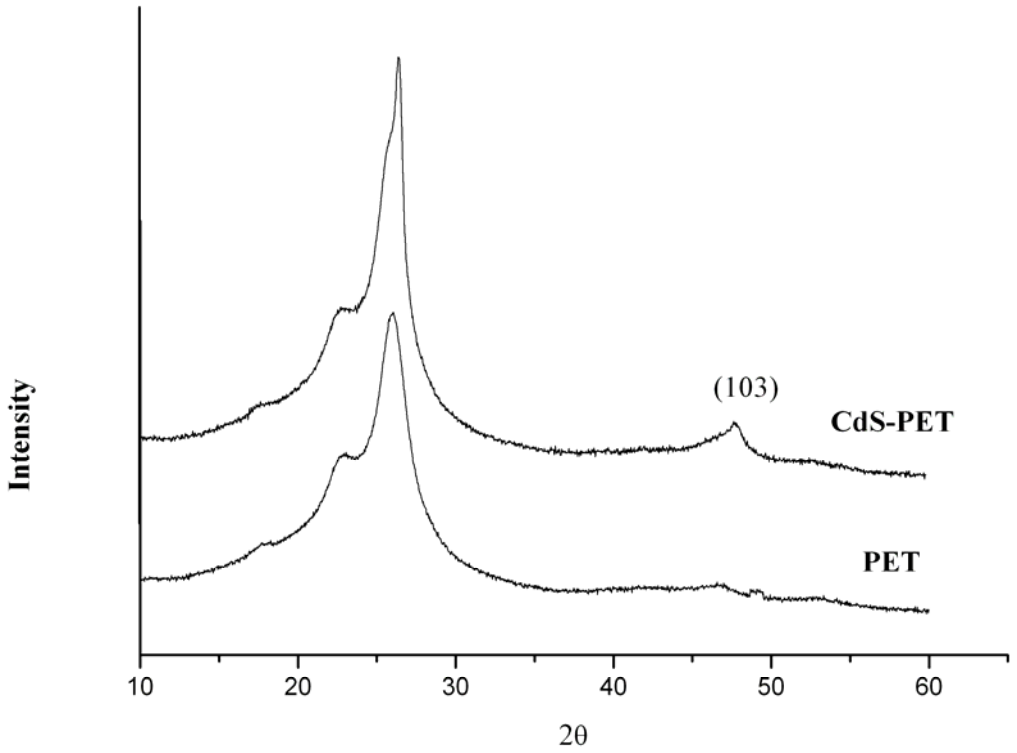

Fig. 2. XRD pattern of PET and CdS-PET film

I-V characteristic of Al/n-CdS junction on PET substrate show the rectification behaviour, which indicates the formation of Schottky contact between Al and CdS film. I-V characteristic of this Schottky junction is shown in figure 3.

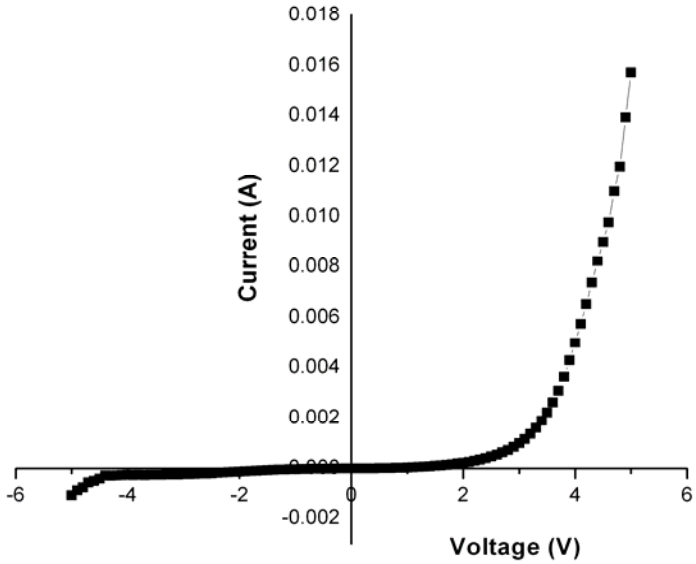

Fig. 3. I-V characteristic of Al/n-CdS Schottky junction at room tempetrture

At low voltage, the current varies exponentially (figure 4) suggesting conduction by thermionic emission [12]. The current through the Schottky junction under low bias voltage (0.0-3.5 V) is given by the following relation

$$I = I_s [\exp (eV/nk_BT) - 1] \quad (2)$$

and

$$I_s = A^* T^2 \exp (-e\Phi_b/k_BT) \quad (3)$$

where e is the charge on electron, V is the applied voltage, n is the diode ideality factor, k_B is the Boltzmann constant, T is the temperature, Φ_b is effective barrier height, A* is effective Richardson constant and I_s is the reverse saturation current.

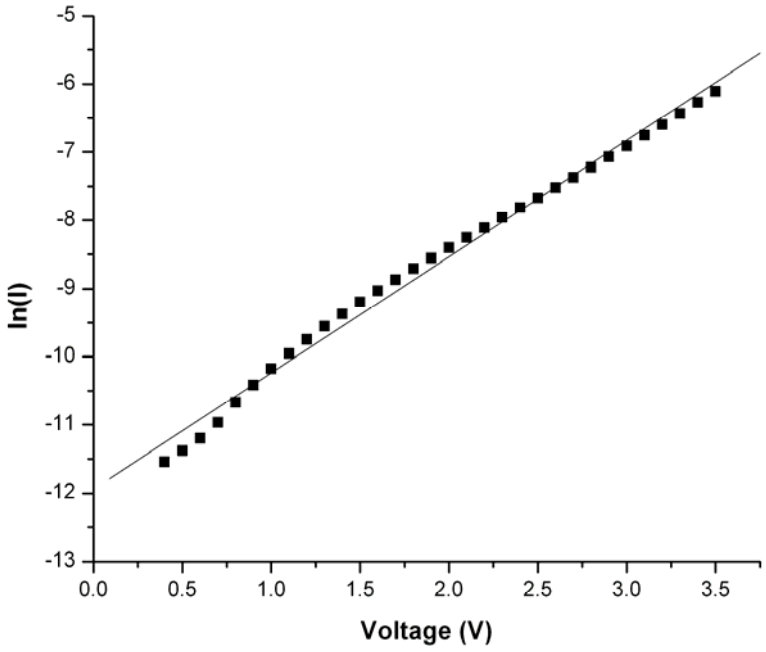

Fig. 4. ln I vs. V curve of Al/n-CdS junction at lower voltages

At voltage above 3.5 V, a non-linear relation ($I \alpha V^2$) of current in Al/CdS junction is obtained as shown in figure 5. This suggests that, in this region, current is controlled by space charge limited conduction (SCLC) [13]. At this biasing voltage, non-linear behavior of Al/n-CdS is also explained by Farag et al [14] using SCLC concept. The observed transition from thermionic to non-linear region of the current with the increase of the biasing voltage usually indicates the onset of a SCLC regime. The current is proportional to V^2 and controlled by the space charge [15] due to the existence of a single discrete set of shallow traps in solids. These traps are responsible for the recombination of the electron-holes generated because of the application of relatively generous higher biasing voltage. In SCLC region, the current can be related to the voltage via the relation

$$I = \frac{\varepsilon_r}{8L^3}\frac{N_C}{N_t} A\mu\varepsilon V^2 \exp\frac{E_t}{kT} \quad (4)$$

where ε_r is the relative permittivity, N_C is the effective density of states, N_t is the concentration of traps with activation energy E_t, L is the film thickness, A is the device area, μ is the mobility and ε is the permittivity.

The reverse saturation current (I_s) is determined by interpolation of exponential slope of I at V=0. The barrier height and ideality factor has been calculated using equation (2) and (3) respectively. It has been found that the reverse saturation current (I_s), barrier height (Φ_b) and ideality factor of Al/n-CdS junction is 4.43 x10^{-5} A, 0.68 eV and 1.24 respectively. The value of ideality factor greater than unity is associated with Fermi-level pinning at the interface [16-20] or relatively large voltage drops in interface region. Interfacial oxide layer may also be the possible cause for a higher ideality factor [21]. Surface defects produce electronic energy levels in the band gaps of CdS semiconductor. These levels can pin the Fermi energy at metal-semiconductor interfaces and cause Schottky-barrier formation [20]. The value of series resistance (R_s) has also been calculated, which is 55.56 Ω for Al/n-CdS junction.

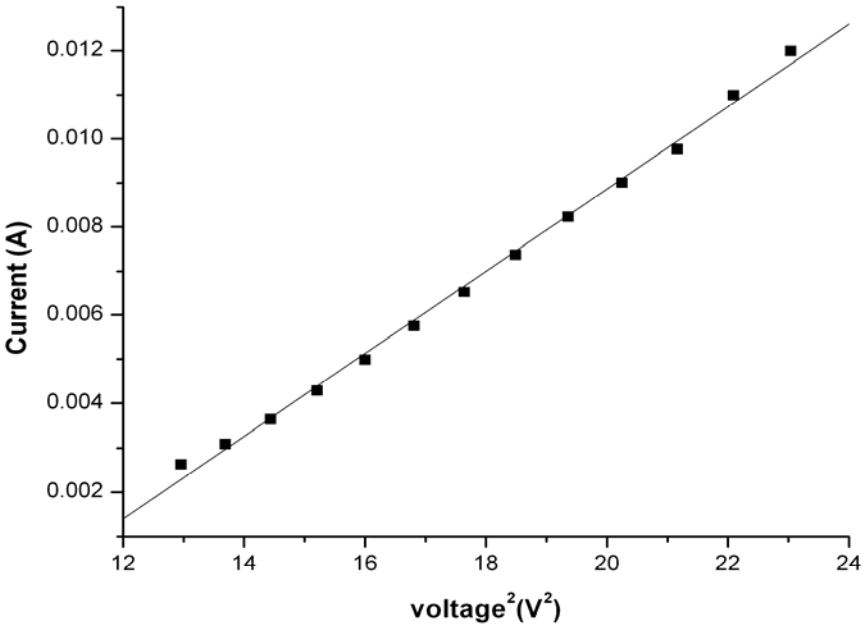

Fig. 5. I vs. V^2 of Al/n-CdS junction at higher voltages

The observed experimental (Schottky) behavior of Al/n-CdS junction is largely attributed to the existence of an electric dipole at the interface of junction [22], which is explained by the proposed band diagram of this junction as shown in figure 6 using tunneling-induced dipole effects. Since the Fermi level of metal is higher than that of semiconductor (shown in figure 6(a)), therefore it is possible that some electron just below the Fermi level in metal can tunnel through the interface into the forbidden gap of semiconductor leaving behind a positive charge on the metal side in the neighborhood of interface. These electrons penetrate a short distance in the semiconductor forbidden band before being reflected back and leave negative charge into the CdS. This creats an electric dipole at the interface for a very short distance, resulting, an upward bending in CdS bands as shown in figure 6(b). To attain equilibrium in this case, electrons move from the conduction band of the semiconductor to the lower available states in the metal. As the electrons leave the semiconductor, they leave behind ionized donors, which shift the semiconductor energies downward until the Fermi levels line up. The charge region of the junction then consists of tunneling-induced dipole layer, a depletion region in the semiconductor and a thin region of charge (in this case positive charge) at the surface of the metal and extends into the metal only to a short distance. Because of relative charge densities in the two materials, virtually the entire voltage drop and space charge region lies within the semiconductor. The barrier for electrons going from the semiconductor to metal is different from the barrier for electrons going from the metal to the semiconductor.

In this band diagram, work function of aluminium (Φ_m) 4.28 eV [23] and work function of n-type CdS material (Φ_s) 4.7 eV [24] have been taken as a standard value, whereas the electron affinity (χ) of CdS is 3.6 eV determined using the relation $\chi = \Phi m - \Phi_b$, values of χ for CdS as reported by different researchers are 4.45 eV [25] and 0.39eV [26]. The built-in potential V_{bi} is the height of Schottky barrier on the semiconductor side, which is equal to the difference between the work function of metal and semiconductor. In this case the value of V_{bi} is 0.42 eV. The band gap of CdS as obtained from optical measurements is 2.41 eV, and is explained below. The carrier density of CdS at surface has been calculated using the formula

$$n = N_c \exp\left(\frac{-e\phi_b}{kT}\right) \quad (5)$$

where Nc is the density of states in conduction band which is equal to 5.66×10^{18} cm^{-3} [27]. The value of carrier density is found to be 2.18×10^{7} cm^{-3}.

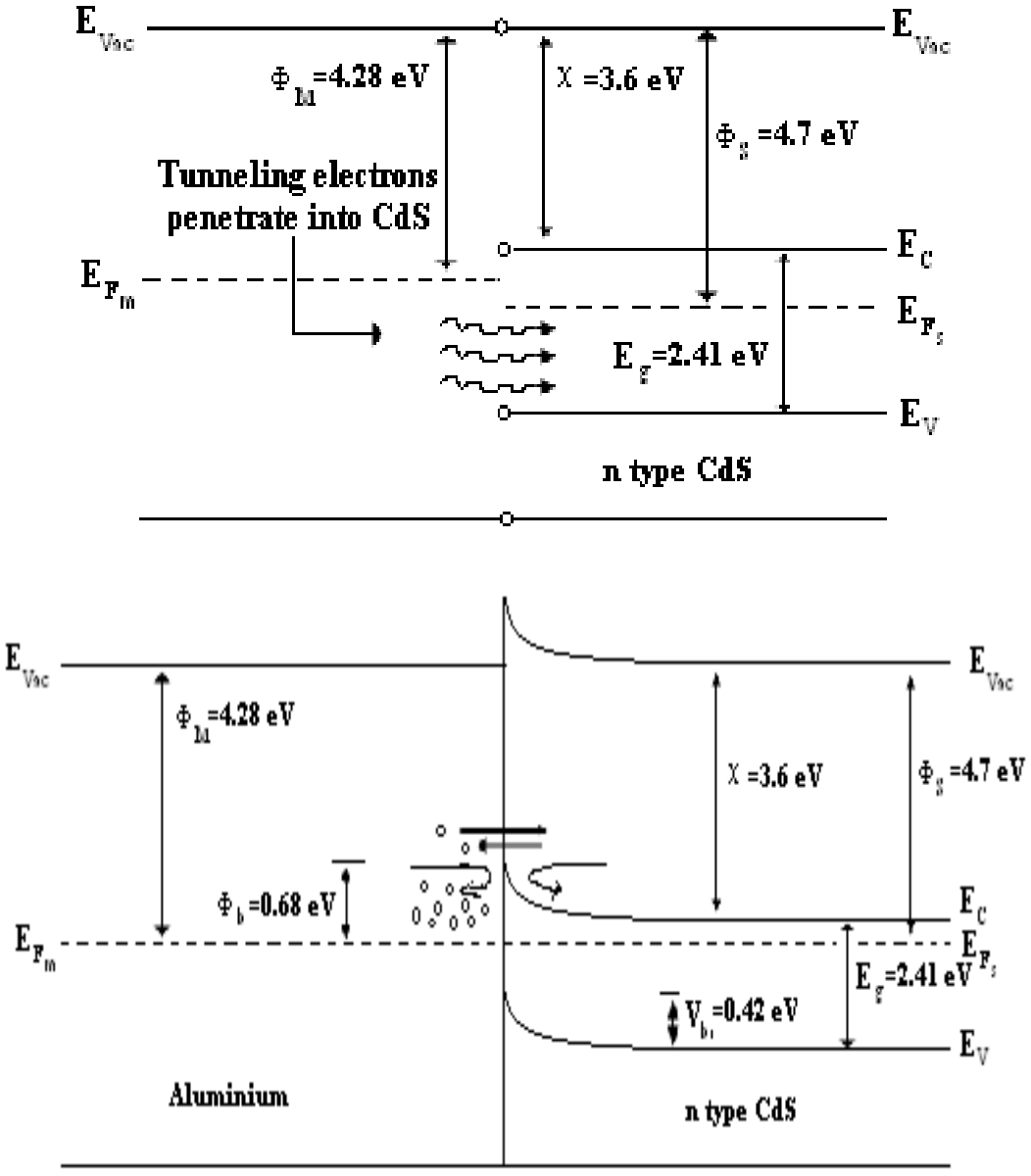

Fig. 6. The energy band diagram of Al/n-CdS Schottky junction including tunneling-induced dipole effect: (a) neutrality (b) equilibrium

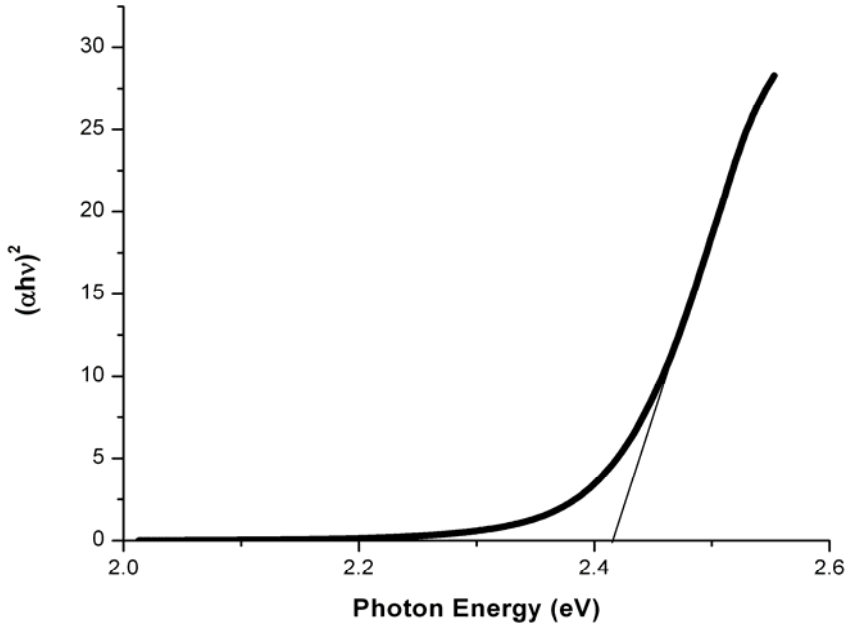

Fig. 7. Energy band gap determination of CdS thin film

From optical absorption spectrum of CdS the band gap was calculated using the Tauc relation [28] given by equation 6.

$$(\alpha\ h\ \nu) = A\ (h\ \nu - E_g)^m \quad (6)$$

where m = ½ for allowed direct transition and A is a constant.
The energy band gap is obtained by plotting a graph between $(\alpha\ h\ \nu)^2$ (as ordinate) and hν (as abscissa) as shown in figure 7. The value of band gap of CdS film is estimated by extrapolating the linear portion of the curve to $(\alpha\ h\ \nu)^2 = 0$. The energy band gap of CdS film is found to be 2.41 eV. The presence of PET film does not affect the absorption spectrum of CdS because it is taken as reference material for the absorption spectrum of CdS film.

4. Conclusion

1. Room temperature deposited CdS film on PET substrate is hexagonal in structure with preferred (103) orientation of micro – crystallites.
2. Al makes Schottky contact with n-CdS. The contact properties such as saturation current, barrier height, ideality factor and series resistance of this junction are 4.43 $x10^{-5}$ A, 0.68 eV, 1.24 and 55.56Ω respectively which helps in the fabrication of Al/n-CdS Schottky junction of particular thickness for their use in electronic devices.
3. At lower bias voltages, current conduction is by thermionic emission where as at higher voltages, current is controlled by SCLC.
4. A band diagram for Al/n-CdS at equilibrium is proposed using tunneling-induced dipole effect at the interface.

Acknowledgments

One of the authors Sandhya Gupta is thankful to UGC for providing financial assistance during this work. Author would also like to thank Ms. Deepika, Ms. Manasvi Dixit and Mr.

Mahesh Baboo, Mr. K.S. Rathore, Mr. Vishal Mathur for their help in various ways during the course of this work.

References

[1] Gupta, S., Patidar, D., Saxena, N. S., Sharma, K., Sharma, T. P. 'Optoelectronics and advanced materials – Rapid communications, **2**, 205 (2008).
[2] Chavez, H., Jorden, M., McClure, J. C., Lush, G., Singh, V. P. 'Physical and electrical characterization of CdS films deposited by vacuum evaporation, solution growth and spray pyrolysis', Journal of material science: Materials in electronics, **8**, 151-154. (1997),
[3] Ferekides, C. S., Marinskiy, D., Marinskaya, S., Tetali, B., Oman, D., Morel, D. L. 'All-CSS processing of CdS/CdTe thin film solar cells with thin CdS layers', IEEE:25th PVSC, 751-756 (1996).
[4] Uda, H., Yonezawa, H., Ohtsubo, Y., Kosaka, M., and Sonomura, H., Solar energy materials and solar cells, **75**, 219 (2003).
[5] Fujita, S., Kawakami, Y., and Fujita, S. 'MO(GS)MBE and photo- MO(GS)MBE of II-VI semiconductors', Journal of Crystal Growth, **164**, 196 (1996),
[6] Pence, S., Bates, C. W., and Varner, L. Materials Letters, **23**, 195 (1995).
[7] Anuar, K., Zulkarnain, Z., Saravanan, N., Nazri, M., and Sharin, R. Materials Science **11**, 101 (2005),
[8] Lee, J. H., Lee, D. J. 'Effects of $CdCl_2$ treatment on the properties of CdS films prepared by r. f. magnetron sputtering', Thin Solid Films, **515**, 6055 (2007).
[9] Mathew, X., Enriquez, J. P., Romeo, A., Tiwari, A. N. Solar energy, **77**, 831 (2004).
[10] Patel, B. K., Nanda, K. K., Sahu, S. N. Journal of Applied Physics, **85**, 3666-3670. (1999),
[11] Latitha, S., Sathyamoorthy, R., Senthilarasu, S., Subbarayan, A., Natarajan, K., Solar energy materials and solar cells, **82**, 187-199. (2004),
[12] Naby, M. A. 'Temperature dependence of I-V and C-V characteristics of Al/CdTe Schottky diodes', Renewable Energy, **6**, 567 (1995),
[13] Wagle, S., and Shirodkar, V., Brazilian Journal of Physics, **30**, 380-385. (2000),
[14] Farag, A. A. M., Yahia, I. S., and Fadel, M. International Journal of Hydrogen Energy, **34**, 4906-4913. (2009),
[15] Balsi, C. D., Micocci, G., Rizzo, A. R., and Tepore, A. Physical Review B, **27**, 2429 (1983),
[16] Brillson, L. J., Physical Review B, **18**, 2431-2446. (1978),
[17] Tersoff, J., Physical Review Letters, **52**, 465-468. (1984),
[18] Tersoff, J., Physical Review B, **32**, 6968-6971. (1985),
[19] Tung, R. T. Physical Review B, **45**, 13509-13523. (1992),
[20] Allen, R. E., Dow, J. D. Physical Review B, **25**, 1423-1426. (1982),
[21] Pattabi, M., Krishnan, S., Ganesh , Mathew, X. 'Effect of temperature and electron irradiation on the I-V characteristics of Au/CdTe Schottky diodes', Solar Energy, **81**, 111 (2007),
[22] Lise, B. Fundamentals of Semiconductor Devices, 1st ed., New York: Mc.Graw Hill, p.331-333(2004),
[23] Mishra, U. K., Singh, J. Semiconductor Device Physics and Design, Netherland: Springer, p. 217 (2008).
[24] Liu, G., Schulmeyer, T., Brotz, J., Klein, A., and Jaegermann, W. Thin Solid Films, 431-432, 477-482 (2003).
[25] Archer, M. D., Hill, R. (2001), Clean electricity from Photovoltaics, UK: Imperial College press, p. 117.
[26] Niles, D. W., Tang, M., McKinley, J., Zanoni, Margaritondo, R. G. Physical Review B, **38**, 10949 (1988),
[27] Sze, S. M. (2002), Semiconductor Devices, 2nd ed., Singapore: John Wiley & Sons.
[28] Tauc, J. (1974), Amorphous & Liquid Semiconductors, New York: Plenum, p.159.